Chapter 3

Actuator and Sensor Models

3.1 Introduction

Actuators and sensors made of piezoelectric material coupons possess desirable properties such as being lightweight, conformable, and having tolerance toward adverse environmental conditions. For these reasons, they are suitable for vibration testing and control, health monitoring, and shape control of a variety of structures. A piezoelectric patch produces strain when a voltage is applied along the poling direction. When this piezoelectric patch is attached to a structure, the strain produced in the patch due to the applied voltage is shared by the structure. This can change the structural shape and can cause motion. This behavior of a piezoelectric patch is termed actuation. The applied voltage on the piezoelectric actuator can be varied according to a control law to obtain desired characteristics in the structural response. Conversely, a piezoelectric material produces voltage when it is subjected to mechanical strain. This property leads to the use of piezoelectric materials as motion sensors.

In this chapter, we extend the derivation presented in the previous chapter to include the actuation and sensing behaviors of piezoelectric patches attached to a shell under pressure. The actuation and sensing properties of a piezoelectric material depend upon how much strain is produced in the material and how much charge a piezoelectric material accumulates when subjected to external voltage and stresses. This can be computed using the constitutive relations for a piezoelectric material, which is presented in the next section. In describing the constitutive relation, important differences between the conventional piezoelectric material and recently developed active composite material are pointed out. A piezoelectric patch brings two types of effects: 1) active effects, i.e., generation of charge and strain due to applied voltage and stress, respectively, and 2) passive effects, i.e., alteration in mass and stiffness of the structure. While the active effects make it possible to use a piezoelectric material as an actuator, or sensor, or both, the passive effects alter the stiffness and mass of the combined structure from that of the original host structure. In most cases, the passive effects are ignored, since the conventional metallic and composite structures are very stiff and heavier compared to the piezoelectric patches. However, inflatable structures are lightweight and have low stiffness, and hence it is important to consider the passive effects of the actuators and sensors. The active and passive effects can be obtained by calculating the changes in the strain energy and the kinetic energy due to piezoelectric patches. This is what is presented after the constitutive relations. Thereafter, the stress resultants and stress couples are calculated for the shell with unimorph and bimorph actuators. Here, we also describe the basic differences between the two types of actuator configurations. After substituting the modified constitutive relations and the inertia terms, we find the equations of motion of a shell under pressure in the presence of piezoelectric actuators. The terms containing the applied voltage are separated to produce the expressions for equivalent actuator forces. A sensor equation is then derived considering an open-circuit configuration. Thereafter, we find the effects of actuators and sensors on individual modes. This is done using the definitions of modal forces and modal sensing constants. At the end, we present a state-space model of the shell attached with actuators and sensors using the modal coordinates and modal velocities as states.

The derivations presented in this chapter are quite general within linear shell theory. As per the need, they can be specialized for different kinds of beams, plates, and shell structures with or without pressure.

3.2 Piezoelectric Constitutive Laws

A piezoelectric material produces strains when an electric field is applied along its poling direction, which is generally along the *3*-direction for a monolithic-type material (Fig. 3.1). Conversely, it generates electric displacement when it is strained. While the former property is used in actuation, the latter is used in sensing. The constitutive relations governing these properties are as follows (IEEE Std, 1978):

$$D_i = d_{ijk} T_{jk} + \varepsilon_{ij}^T E_j$$

$$S_{ij} = s_{ijk}^E T_{kl} + d_{kij} E_k \tag{3.1}$$

where the indices i, j, k vary from *1* to *3*, D_i is the electric displacement (charge per unit area), d_{ijk} is the piezoelectric strain tensor, T_{jk} is the stress tensor, ε_{ij}^T is the permitivity tensor measured at a constant stress, E_k is the electric field, S_{ij} is the mechanical strain tensor, and s_{ijk}^E is the elastic compliance tensor measured at a constant electric field. By discarding all the quantities related to piezoelectricity in the above equation, one could obtain the constitutive relations for a conventional (non-piezoelectric) material. In Eqs. (3.1), the first and the second equations describe the sensing and actuation phenomena of a piezoelectric material, respectively. A conventional monolithic piezoelectric material demonstrates in-plane isotropy. This makes its modeling easier compared to the recently developed non-isotropic composite actuators and sensors, e.g., Active Fiber Composite (AFC) actuator and Macro-Fiber Composite (MFC^{TM}) actuator (Fig. 3.2; Wilkie, 2000). However, these active composites have several advantages, such as high electro-mechanical

coupling, more flexibility, and improved damage tolerance. Moreover, the composite actuators can also produce twisting motions, which is difficult to achieve using a conventional piezoelectric material. In a conventional piezoelectric actuator, the direction of the applied electric field is perpendicular to the induced in-plane strains, leading to smaller electro-mechanical coupling. On the other hand, in a composite actuator, the piezoceramic fibers and electrodes are placed in such a way that the electric field coincides with the direction of induced strain along a preferred direction. This leads to a higher direction-dependent electro-mechanical coupling.

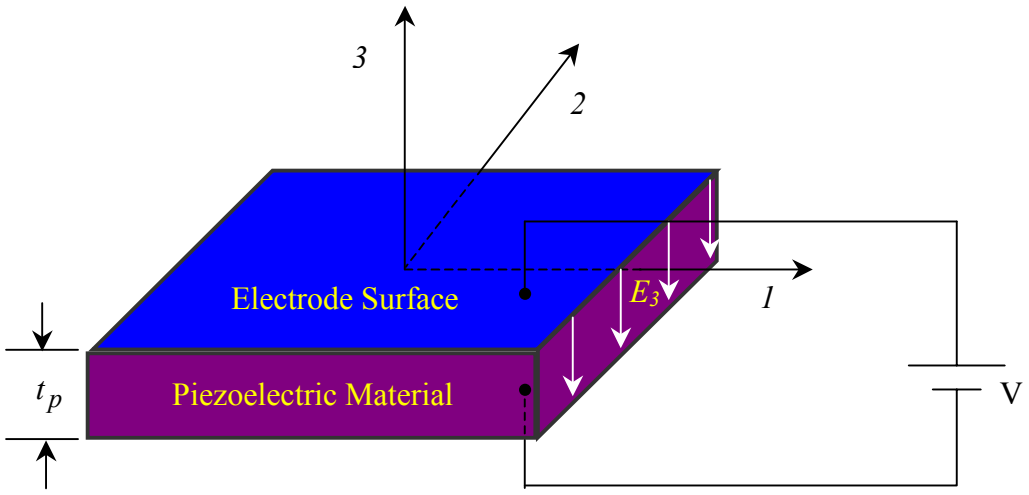

Fig. 3.1: A monolithic piezoelectric wafer with coordinate system

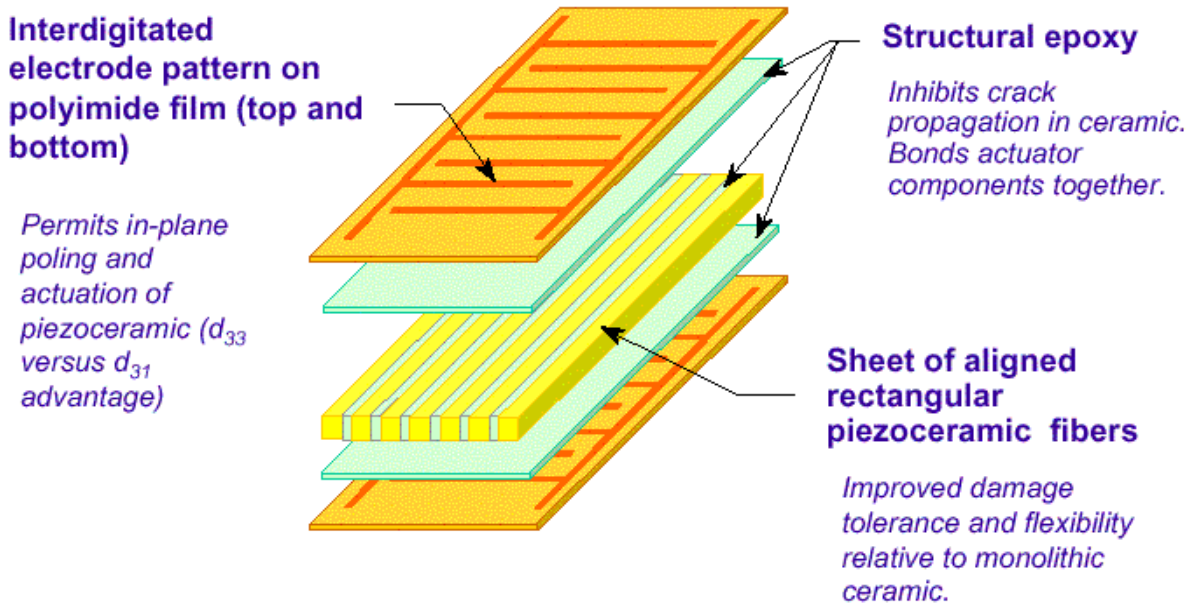

Fig. 3.2: Components of Macro-Fiber Composite™ (Wilkie et al. 2000).

Composite actuators are generally made of piezoceramic fibers, interdigitated electrodes, and a polymer matrix (Fig. 3.2). The fiber-reinforced materials are often characterized as orthotropic with the fiber direction as one of the three principal material directions (Reddy, 1996). Thus, the piezo-elastic properties of these composites can be described by assuming an orthorhombic piezoelectric crystal structure with orthotropic structural properties. For such a material, Eqs. (3.1) can be expanded as

$$\begin{Bmatrix} D_1 \\ D_2 \\ D_3 \end{Bmatrix} = \begin{bmatrix} 0 & 0 & 0 & 0 & d_{15} & 0 \\ 0 & 0 & 0 & d_{24} & 0 & 0 \\ d_{31} & d_{32} & d_{33} & 0 & 0 & 0 \end{bmatrix} \begin{Bmatrix} T_{11} \\ T_{22} \\ T_{33} \\ T_{23} \\ T_{13} \\ T_{12} \end{Bmatrix} + \begin{bmatrix} \varepsilon_{11}^T & 0 & 0 \\ 0 & \varepsilon_{22}^T & 0 \\ 0 & 0 & \varepsilon_{33}^T \end{bmatrix} \begin{Bmatrix} E_1 \\ E_2 \\ E_3 \end{Bmatrix}$$

$$\begin{Bmatrix} S_{11} \\ S_{22} \\ S_{33} \\ S_{23} \\ S_{13} \\ S_{12} \end{Bmatrix} = \begin{bmatrix} \frac{1}{E_1^p} & -\frac{\nu_{21}^p}{E_2^p} & -\frac{\nu_{31}^p}{E_3^p} & 0 & 0 & 0 \\ -\frac{\nu_{12}^p}{E_1^p} & \frac{1}{E_2^p} & -\frac{\nu_{32}^p}{E_3^p} & 0 & 0 & 0 \\ -\frac{\nu_{13}^p}{E_1^p} & -\frac{\nu_{23}^p}{E_2^p} & \frac{1}{E_3^p} & 0 & 0 & 0 \\ 0 & 0 & 0 & \frac{1}{G_{23}^p} & 0 & 0 \\ 0 & 0 & 0 & 0 & \frac{1}{G_{13}^p} & 0 \\ 0 & 0 & 0 & 0 & 0 & \frac{1}{G_{12}^p} \end{bmatrix} \begin{Bmatrix} T_{11} \\ T_{22} \\ T_{33} \\ T_{23} \\ T_{13} \\ T_{12} \end{Bmatrix} + \begin{bmatrix} 0 & 0 & d_{31} \\ 0 & 0 & d_{32} \\ 0 & 0 & d_{33} \\ 0 & d_{24} & 0 \\ d_{15} & 0 & 0 \\ 0 & 0 & 0 \end{bmatrix} \begin{Bmatrix} E_1 \\ E_2 \\ E_3 \end{Bmatrix}$$

(3.2)

where E_1^p, E_2^p, and E_3^p are the elastic moduli, G_{23}^p, G_{13}^p, and G_{12}^p are the shear moduli, and ν_{21}^p, ν_{31}^p, ν_{12}^p, ν_{32}^p, ν_{13}^p, and ν_{23}^p are Poisson's ratios of the piezoelectric material. The six Poisson's ratios are not independent but rather constrained to follow the relations:

$$\frac{\nu_{21}^p}{E_2^p} = \frac{\nu_{12}^p}{E_1^p}, \qquad \frac{\nu_{31}^p}{E_3^p} = \frac{\nu_{13}^p}{E_1^p}, \qquad \frac{\nu_{32}^p}{E_3^p} = \frac{\nu_{23}^p}{E_2^p} \tag{3.3}$$

Equations (3.2) can be simplified by using the facts that the electric field will be applied in only the *3*-direction and T_{33} and S_{33} can be neglected according to Love's first approximation. We also note that for a thin shell, the shear stress in the *3*-direction will be very small and hence the electric displacement in the *1*- and *2*- directions will be very small. Making these simplifications in Eqs. (3.2) and denoting the stresses (T_{jk}) and strains (S_{ij}) by the usual notations of the theory of elasticity, we get

$$D_3 = d_{31}\sigma_{11}^p + d_{32}\sigma_{22}^p + \varepsilon_{33}^T E_3$$

$$\begin{Bmatrix} \varepsilon_{11}^p \\ \varepsilon_{22}^p \\ \gamma_{23}^p \\ \gamma_{13}^p \\ \gamma_{12}^p \end{Bmatrix} = \begin{bmatrix} \frac{1}{E_1^p} & -\frac{\nu_{21}^p}{E_2^p} & 0 & 0 & 0 \\ -\frac{\nu_{12}^p}{E_1^p} & \frac{1}{E_2^p} & 0 & 0 & 0 \\ 0 & 0 & \frac{1}{G_{23}^p} & 0 & 0 \\ 0 & 0 & 0 & \frac{1}{G_{13}^p} & 0 \\ 0 & 0 & 0 & 0 & \frac{1}{G_{12}^p} \end{bmatrix} \begin{Bmatrix} \sigma_{11}^p \\ \sigma_{22}^p \\ \sigma_{23}^p \\ \sigma_{13}^p \\ \sigma_{12}^p \end{Bmatrix} + \begin{bmatrix} d_{31} \\ d_{32} \\ 0 \\ 0 \\ 0 \end{bmatrix} E_3 \tag{3.4}$$

Equation (3.4) will be used in deriving the actuator and sensor equations. So far, we used the sign convention suitable for a monolithic piezoelectric material. For an active composite material, there would be a slight change in the notation for the piezoelectric quantities of Eq. (3.4). In the case of an active composite material, the poling direction is along the *1*-axis (fiber direction) instead of the *3*-axis. Hence, the symbols d_{31}, d_{32}, ε_{33}^{T}, and E_3 should be changed to d_{11}, d_{12}, ε_{11}^{T}, and E_1 when using Eq. (3.4) for an active composite material. However, we will continue using the sign convention of a monolithic, keeping in mind these notation differences. In Eqs. (3.4), σ_{11}^{p} and σ_{22}^{p} are the normal stresses along α_1 and α_2 directions, ε_{11}^{p} and ε_{22}^{p} are the corresponding normal strains, σ_{23}^{p}, σ_{13}^{p}, σ_{12}^{p} are shearing stresses, and γ_{23}^{p}, γ_{13}^{p}, γ_{12}^{p} are the corresponding engineering shearing strains in the piezoelectric patches. Solving Eqs. (3.4) for stresses yields

$$\begin{Bmatrix} \sigma_{11}^{p} \\ \sigma_{22}^{p} \\ \sigma_{23}^{p} \\ \sigma_{13}^{p} \\ \sigma_{12}^{p} \end{Bmatrix} = \begin{bmatrix} \dfrac{E_1^{p}}{1-\nu_{12}^{p}\nu_{21}^{p}} & \dfrac{\nu_{21}^{p}E_1^{p}}{1-\nu_{12}^{p}\nu_{21}^{p}} & 0 & 0 & 0 \\ \dfrac{\nu_{21}^{p}E_1^{p}}{1-\nu_{12}^{p}\nu_{21}^{p}} & \dfrac{E_2^{p}}{1-\nu_{12}^{p}\nu_{21}^{p}} & 0 & 0 & 0 \\ 0 & 0 & G_{23}^{p} & 0 & 0 \\ 0 & 0 & 0 & G_{13}^{p} & 0 \\ 0 & 0 & 0 & 0 & G_{12}^{p} \end{bmatrix} \begin{Bmatrix} \varepsilon_{11}^{p} \\ \varepsilon_{22}^{p} \\ \gamma_{23}^{p} \\ \gamma_{13}^{p} \\ \gamma_{12}^{p} \end{Bmatrix} - \begin{bmatrix} \dfrac{E_1^{p}(d_{31}+\nu_{21}^{p}d_{32})}{1-\nu_{12}^{p}\nu_{21}^{p}} \\ \dfrac{E_2^{p}(d_{32}+\nu_{12}^{p}d_{31})}{1-\nu_{12}^{p}\nu_{21}^{p}} \\ 0 \\ 0 \\ 0 \end{bmatrix} E_3 \tag{3.5}$$

In deriving Eqs. (3.5), we used the fact that

$$\nu_{12}^{p}E_2^{p} = \nu_{21}^{p}E_1^{p} \tag{3.6}$$

While the above equations are written for an active composite material, simplifications for a monolithic PZT can be obtained by substituting $E_1^{p} = E_2^{p} = E^{p}$,

$G_{12}^p = G_{23}^p = G_{13}^p = G^p$, and $\nu_{21}^p = \nu_{12}^p = \nu^p$. The electric field applied to the actuator is generated by a voltage source. The relationship between the two is as follows

$$E_3 = \frac{V}{t} \tag{3.7}$$

where, for a monolithic piezoelectric actuator, t is the thickness of the actuator (Fig. 3.1) and, for AFC/ MFC^{TM}, t is the spacing between the interdigitated electrode (Fig 3.2).

3.3 Changes in Energy Terms due to Piezoelectric Patches

The active and the passive effects of piezoelectric patches can be obtained by calculating the changes in strain energy and the kinetic energy of the host structure due to addition of the piezoelectric patches. Then, the composite equations of motion of the combined structure can be derived using Hamilton's principle, as done in the second chapter for the shell without any patches. In this section, we derive these additional energy terms. Before we embark on finding these energy terms, we define the so-called distribution function to distinguish the regions with and without patches. A distribution function will be nonzero only for those locations of the shell where a patch is attached. We assume that the number of patch layers is the same wherever patches are attached. If the shell has a different number of patches at different locations, the distribution function will have to be modified accordingly. We assume that the patches are of the shape of generalized rectangle in the curvilinear coordinate system given by α_1 and α_2. This means that the shape of a patch can be given by the coordinates of its four corners. Since there could be more than one patch in general, we define the distribution function $\Delta_p(\alpha_1, \alpha_2)$ as

$$\Delta_p(\alpha_1, \alpha_2) = \sum_{m=1}^{N_a} \{H(\alpha_1 - \alpha_{11}^m) - H(\alpha_1 - \alpha_{12}^m)\}\{H(\alpha_2 - \alpha_{21}^m) - H(\alpha_2 - \alpha_{22}^m)\}, \tag{3.8}$$

where $H(x-x_1)$ is the Heaviside function defined as

$$H(x-x_1)=\begin{cases}1; & x \geq x_1 \\ 0; & x < x_1\end{cases}. \tag{3.9}$$

In Eq. (3.8), α_{11}^m, α_{12}^m define the extent of the actuator along the α_1 coordinate and α_{21}^m, α_{22}^m define the extent along the α_2 coordinate, *m* is an index, and N_a is the total number of actuators.

3.3.1 Strain Energy

We assume that the bonding between the core and piezoelectric layer is perfect and of zero thickness. We derived the strain energy for the shell under pressure in previous chapter. A similar expression for the strain energy of the piezoelectric patches can be written as

$$\Delta P=\frac{1}{2}(\sigma_{11}^p\varepsilon_{11}+\sigma_{22}^p\varepsilon_{22}+\sigma_{23}^p\gamma_{23}+\sigma_{13}^p\gamma_{13}+\sigma_{12}^p\gamma_{12}). \tag{3.10}$$

where $\varepsilon_{11}=\varepsilon_{11}^p-d_{31}E_3$, $\varepsilon_{22}=\varepsilon_{22}^p-d_{32}E_3$, $\gamma_{23}=\gamma_{23}^p$, $\gamma_{13}=\gamma_{13}^p$, and $\gamma_{12}=\gamma_{12}^p$. In writing Eqs. (3.10), we ignored the initial stresses in the patches since the changes in the initial stress resultants due to the addition of patches will be small. With the new strain definitions, the constitutive relations can be written as

$$\begin{Bmatrix} \sigma_{11}^p \\ \sigma_{22}^p \\ \sigma_{23}^p \\ \sigma_{13}^p \\ \sigma_{12}^p \end{Bmatrix} = \begin{bmatrix} \frac{E_1^p}{1-\nu_{12}^p \nu_{21}^p} & \frac{\nu_{21}^p E_1^p}{1-\nu_{12}^p \nu_{21}^p} & 0 & 0 & 0 \\ \frac{\nu_{21}^p E_1^p}{1-\nu_{12}^p \nu_{21}^p} & \frac{E_2^p}{1-\nu_{12}^p \nu_{21}^p} & 0 & 0 & 0 \\ 0 & 0 & G_{23}^p & 0 & 0 \\ 0 & 0 & 0 & G_{13}^p & 0 \\ 0 & 0 & 0 & 0 & G_{12}^p \end{bmatrix} \begin{Bmatrix} \varepsilon_{11} \\ \varepsilon_{22} \\ \gamma_{23} \\ \gamma_{23} \\ \gamma_{12} \end{Bmatrix} \tag{3.11}$$

From Eq (3.11), we can find the derivative of ΔP with respect to ε_{11} as

$$\frac{\partial \Delta P}{\partial \varepsilon_{11}} = \frac{1}{2}(\sigma_{11}^p + \frac{E_1^p}{1-\nu_{12}^p \nu_{21}^p}\varepsilon_{11} + \frac{\nu_{12}^p E_2^p}{1-\nu_{12}^p \nu_{21}^p}\varepsilon_{22}) = \sigma_{11}^p . \tag{3.12}$$

Similarly, other derivatives of ΔP can be calculated. Summarizing, we get

$$\frac{\partial \Delta P}{\partial \varepsilon_{11}} = \sigma_{11}^p, \quad \frac{\partial \Delta P}{\partial \varepsilon_{22}} = \sigma_{22}^p, \quad \frac{\partial \Delta P}{\partial \gamma_{23}} = \sigma_{23}^p, \quad \frac{\partial \Delta P}{\partial \gamma_{13}} = \sigma_{13}^p \quad \frac{\partial \Delta P}{\partial \gamma_{12}} = \sigma_{12}^p . \tag{3.13}$$

This leads to the following change in the expression for the variation of strain energy due to a piezoelectric patch:

$$\delta \Delta U = \int_{V_p} [\sigma_{11}^p \delta\varepsilon_{11} + \sigma_{22}^p \delta\varepsilon_{22} + \sigma_{23}^p \delta\gamma_{23} + \sigma_{13}^p \delta\gamma_{13} + \sigma_{12}^p \delta\gamma_{12}] dV , \tag{3.14}$$

where V_p is the volume of the material in the piezoelectric patches. Eq. (3.14) can be used in deriving the equations of motion due of the shell attached with the piezoelectric actuators. While the stiffness of the actuator will contribute to the passive effect, the terms corresponding to the electric field will give the active effect.

3.3.2 Kinetic Energy

Now we find how the kinetic energy and hence the inertia terms change due to the addition of the piezoelectric patches. To this end, we modify the kinetic energy by adding the following:

$$\Delta K_E = \tfrac{1}{2} \int_{V_p} \rho_p \, (\dot{U}_1 \boldsymbol{t}_1 + \dot{U}_2 \boldsymbol{t}_2 + \dot{W} \boldsymbol{t}_3) \cdot (\dot{U}_1 \boldsymbol{t}_1 + \dot{U}_2 \boldsymbol{t}_2 + \dot{W} \boldsymbol{t}_3) \, dV_p \,, \tag{3.15}$$

where ρ_p is the density of the piezoelectric material. Following the same procedure as adopted for the shell and noting that the domain of the second integral is only the volume of the material in the piezoelectric patches, we get

$$\int_{t_o}^{t_1} \delta \Delta K_E \, dt = -\Delta_p \, (\alpha_1, \alpha_2) \rho_p \, h_p \int_{t_o}^{t_1} \int_{\alpha_2} \int_{\alpha_1} [(\ddot{u}_1 \, \delta u_1 + \ddot{u}_2 \, \delta u_2 + \ddot{w} \, \delta w)] \, A_1 \, A_2 \; d\alpha_1 \, d\alpha_2 \, dt \,, \tag{3.16}$$

where h_p is the thickness of the patches that has been assumed constant for all patches, and t_o, t_1 are initial and final times. The above equation suggests that the term ρh in the original shell equation should be changed to $\rho h + \Delta_p \, \rho_p \, h_p$ in order to take into account the mass of the piezoelectric patches.

3.4 Stress Resultants and Stress Couples

3.4.1 General Forms

The equations of motion (except the inertia terms) for a shell with patches can be derived by adding the stress resultants due to patches to the stress resultants of the shell. The stress resultants and stress couples in any region - patch or no patch - can be given by

$$\begin{Bmatrix} N_{11} \\ N_{12} \\ Q_{13} \end{Bmatrix} = \sum_{k=1}^{n} \int_{h_{k-1}}^{h_k} \begin{Bmatrix} \sigma_{11} \\ \sigma_{12} \\ \sigma_{13} \end{Bmatrix}_k (1+\frac{\zeta}{R_2}) d\zeta \,, \qquad \begin{Bmatrix} N_{22} \\ N_{21} \\ Q_{23} \end{Bmatrix} = \sum_{k=1}^{n} \int_{h_{k-1}}^{h_k} \begin{Bmatrix} \sigma_{22} \\ \sigma_{21} \\ \sigma_{23} \end{Bmatrix}_k (1+\frac{\zeta}{R_1}) d\zeta \,,$$

$$\begin{Bmatrix} M_{11} \\ M_{12} \end{Bmatrix} = \sum_{k=1}^{n} \int_{h_{k-1}}^{h_k} \begin{Bmatrix} \sigma_{11} \\ \sigma_{12} \end{Bmatrix}_k \zeta\,(1+\frac{\zeta}{R_2}) d\zeta \,, \qquad \begin{Bmatrix} M_{22} \\ M_{21} \end{Bmatrix} = \sum_{k=1}^{n} \int_{h_{k-1}}^{h_k} \begin{Bmatrix} \sigma_{22} \\ \sigma_{21} \end{Bmatrix}_k \zeta\,(1+\frac{\zeta}{R_1}) d\zeta \,, \tag{3.17}$$

where N_{ij} are the total in-plane stress resultants, Q_{i3} are the total transverse shear stress resultants, and M_{ij} are the total moment resultants. The indices i and j take values *1* and *2*, n denotes the number of layers including the shell and the patches, and h_{k-1} and h_k are the distances of the lower and the upper surface of the k^{th} layer from the reference surface, respectively. Usually, two types of configuration of patches are considered (Fig. 3.3). One is a bimorph configuration where one actuator is attached to the top surface and the other to the bottom, and the second is a unimorph configuration where there is only one actuator layer (either on the top or the on bottom). In the above equation, the value of *n* would be *1* for the region where there is no patch attached, *2* for the patch region with unimorph configuration, and *3* for a patch region with bimorph configuration. For convenience of writing, the total stress resultants and stress couples are broken into three parts, of which the last two will be zero for the regions where there is no patch attached:

$$\begin{Bmatrix} N_{11} \\ N_{12} \\ Q_{13} \end{Bmatrix} = \begin{Bmatrix} N_{11}^{t} \\ N_{12}^{t} \\ Q_{13}^{t} \end{Bmatrix} + \begin{Bmatrix} N_{11}^{p} \\ N_{12}^{p} \\ Q_{13}^{p} \end{Bmatrix} + \begin{Bmatrix} N_{11}^{E} \\ 0 \\ 0 \end{Bmatrix}, \qquad \begin{Bmatrix} N_{22} \\ N_{21} \\ Q_{23} \end{Bmatrix} = \begin{Bmatrix} N_{22}^{t} \\ N_{21}^{t} \\ Q_{23}^{t} \end{Bmatrix} + \begin{Bmatrix} N_{22}^{p} \\ N_{21}^{p} \\ Q_{23}^{p} \end{Bmatrix} + \begin{Bmatrix} N_{22}^{E} \\ 0 \\ 0 \end{Bmatrix},$$

$$\begin{Bmatrix} M_{11} \\ M_{12} \end{Bmatrix} = \begin{Bmatrix} M_{11}^{t} \\ M_{12}^{t} \end{Bmatrix} + \begin{Bmatrix} M_{11}^{p} \\ M_{12}^{p} \end{Bmatrix} + \begin{Bmatrix} M_{11}^{E} \\ 0 \end{Bmatrix}, \qquad \begin{Bmatrix} M_{22} \\ M_{21} \end{Bmatrix} = \begin{Bmatrix} M_{22}^{t} \\ M_{21}^{t} \end{Bmatrix} + \begin{Bmatrix} M_{22}^{p} \\ M_{21}^{p} \end{Bmatrix} + \begin{Bmatrix} M_{22}^{E} \\ 0 \end{Bmatrix}. \tag{3.18}$$

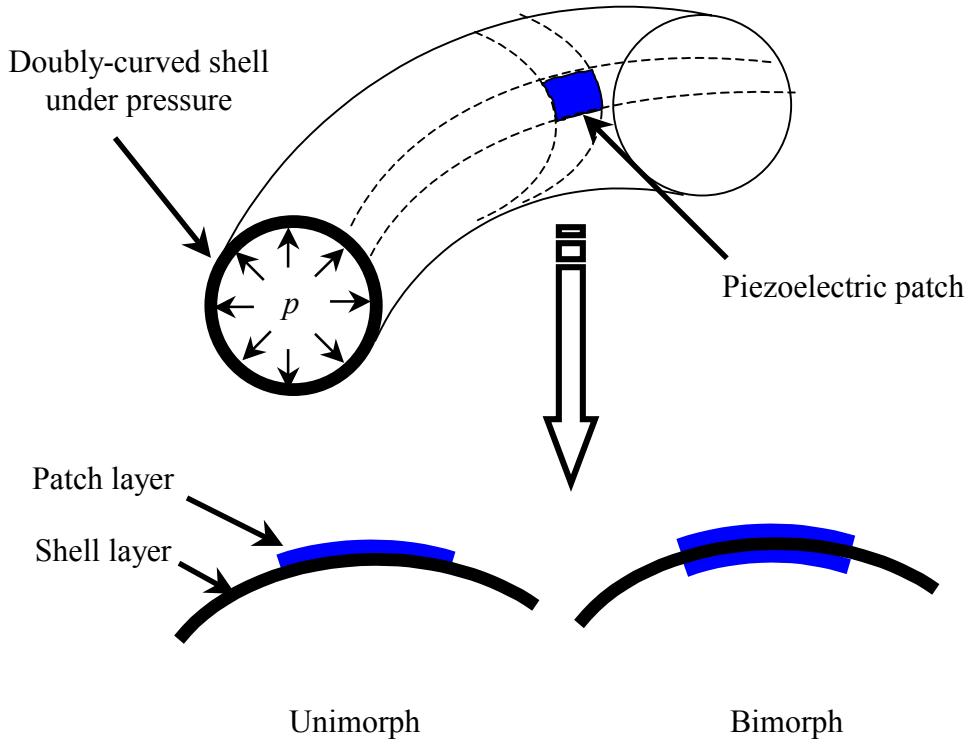

Fig. 3.3: Shell with unimorph and bimorph patches.

The modified shear stress resultants defined by Sanders can be obtained similar to the modified shear stress resultants of the shell given in Eqs. (2.68). The right-hand-sides of the above equations consist of three groups. The terms in the first two groups are due to the structural stiffness of the shell and the patch and the third group of terms are due to the voltage applied on the patch. When these constitutive equations are substituted in the

equations of motion and the terms corresponding to the electric fields are separated, the equations of motion of the complete structure and the generalized forces produced by the piezoelectric patches are obtained. The terms in Eqs. (3.18) will be different for unimorph and bimorph configurations. The general forms are given below:

$$\begin{Bmatrix} N_{11}^{\alpha} \\ N_{22}^{\alpha} \\ \tilde{N}_{12}^{\alpha} \end{Bmatrix} = \begin{bmatrix} A_{11}^{\alpha} & A_{12}^{\alpha} & 0 \\ A_{12}^{\alpha} & A_{22}^{\alpha} & 0 \\ 0 & 0 & A_{66}^{\alpha} \end{bmatrix} \begin{Bmatrix} \varepsilon_{11} \\ \varepsilon_{22} \\ \gamma_{12} \end{Bmatrix} + \begin{bmatrix} B_{11}^{\alpha} & B_{12}^{\alpha} & 0 \\ B_{12}^{\alpha} & B_{22}^{\alpha} & 0 \\ 0 & 0 & B_{66}^{\alpha} \end{bmatrix} \begin{Bmatrix} \kappa_{11} \\ \kappa_{22} \\ 2\tilde{\kappa}_{12} \end{Bmatrix},$$

$$\begin{Bmatrix} M_{11}^{\alpha} \\ M_{22}^{\alpha} \\ \tilde{M}_{12}^{\alpha} \end{Bmatrix} = \begin{bmatrix} B_{11}^{\alpha} & B_{12}^{\alpha} & 0 \\ B_{12}^{\alpha} & B_{22}^{\alpha} & 0 \\ 0 & 0 & B_{66}^{\alpha} \end{bmatrix} \begin{Bmatrix} \varepsilon_{11} \\ \varepsilon_{22} \\ \gamma_{12} \end{Bmatrix} + \begin{bmatrix} D_{11}^{\alpha} & D_{12}^{\alpha} & 0 \\ D_{12}^{\alpha} & D_{22}^{\alpha} & 0 \\ 0 & 0 & D_{66}^{\alpha} \end{bmatrix} \begin{Bmatrix} \kappa_{11} \\ \kappa_{22} \\ 2\tilde{\kappa}_{12} \end{Bmatrix}, \tag{3.19}$$

where the superscript α can be replaced by either t or p to get the terms in the first two groups of Eqs. (3.18). The last groups of terms will have the following forms:

$$\begin{Bmatrix} N_{11}^{E} \\ N_{22}^{E} \end{Bmatrix} = \begin{Bmatrix} A_{11}^{E} \\ A_{22}^{E} \end{Bmatrix} \Delta_E, \qquad \begin{Bmatrix} M_{11}^{E} \\ M_{22}^{E} \end{Bmatrix} = \begin{Bmatrix} D_{11}^{E} \\ D_{22}^{E} \end{Bmatrix} \Delta_E, \tag{3.20}$$

where $\Delta_E(\alpha_1, \alpha_2)$, which includes the locations of the patches as well as the electric field applied to each of them, is defined as

$$\Delta_E(\alpha_1, \alpha_2) = \sum_{m=1}^{N_a} \{H(\alpha_1 - \alpha_{11}^m) - H(\alpha_1 - \alpha_{12}^m)\} \{H(\alpha_2 - \alpha_{21}^m) - H(\alpha_2 - \alpha_{22}^m)\} E_3^m \tag{3.21}$$

In the above equation, E_3^m is the applied electric field on the m^{th} actuator. Now we present the elements of the matrices of Eqs. (3.19) and (3.20) for unimorph and bimorph configurations.

3.4.2 Bare Shell

By a bare shell, we mean the parts of the shell where there is no patch attached. Since there is no patch, only the terms of the first group in Eqs. (3.18) will be nonzero. Elements of the corresponding matrices of Eqs. (3.19) are

$$A_{11}^t = \frac{E\,h}{1-\nu^2}, \qquad A_{12}^t = \nu\, A_{11}^t, \qquad A_{22}^t = A_{11}^t, \qquad A_{66}^t = G\,h$$

$$B_{11}^t = B_{12}^t = B_{22}^t = B_{66}^t = 0$$

$$D_{11}^t = \frac{E\,h^3}{12(1-\nu^2)}, \qquad D_{12}^t = \nu\, D_{11}^t, \qquad D_{22}^t = D_{11}^t, \qquad D_{66}^t = \frac{G\,h^3}{12}$$

(3.22)

3.4.3 Unimorph Configuration

As mentioned before, in a unimorph configuration, the patch is attached to only one side of the shell. In this case, the neutral surface shifts from the mid-surface of the shell due to the single layer of the patch. Assuming that the patch is attached to the upper surface, the distance, h_c, of the neutral surface from the lower surface of the shell is

$$h_c = \frac{E^p h_p^2 + 2E^p h_p h + E\,h^2}{2E^p h_p + 2E\,h}. \tag{3.23}$$

where E^p is either E_1^p or E_2^p depending upon the direction of stress resultant and couples. The elements of Eq. (3.19) are

$$A_{11}^t = \frac{E\,h}{1-\nu^2}, \qquad A_{12}^t = \nu\, A_{11}^t, \qquad A_{22}^t = A_{11}^t, \qquad A_{66}^t = G\,h,$$

$$B_{11}^t = \frac{E\,h(h-2h_c)}{2(1-\nu^2)}, \qquad B_{12}^t = \nu\, B_{11}^t, \qquad B_{22}^t = B_{11}^t, \qquad B_{66}^t = \frac{G\,h(h-2h_c)}{2},$$

$$D_{11}^t = \frac{E\,h(3h_c^2 - 3h\,h_c + h^2)}{3(1-\nu^2)}, \qquad D_{12}^t = \nu\, D_{11}^t, \quad D_{22}^t = D_{11}^t, \quad D_{66}^t = \frac{G\,h(6h_c^2 - 6\,h_c h + 2h^2)}{6},$$

$$A_{11}^p = \frac{E_1^p\, h_p}{1-\nu_{12}^p \nu_{21}^p}, \qquad A_{12}^p = \nu_{21}^p\, A_{11}^p, \qquad A_{22}^p = \frac{E_2^p\, h_p}{1-\nu_{12}^p \nu_{21}^p}, \qquad A_{66}^t = G_{12}^p\, h_p,$$

$$B_{11}^p = \frac{E_1^p\, h_p\,(-2h_c + 2h + h_p)}{2(1-\nu_{12}^p \nu_{21}^p)}, \qquad B_{12}^p = \nu_{21}^p\, B_{11}^p,$$

$$B_{22}^p = \frac{E_2^p\, h_p\,(-2h_c + 2h + h_p)}{2(1-\nu_{12}^p \nu_{21}^p)}, \qquad B_{66}^t = \frac{G_{12}^p\, h_p\,(-2h_c + 2h + h_p)}{2},$$

$$D_{11}^p = \frac{E_1^p\,\{(h_c - h)^3 + (-h_c + h + h_p)^3\}}{3(1-\nu_{12}^p \nu_{21}^p)}, \qquad D_{12}^p = \nu_{21}^p\, D_{11}^p,$$

$$D_{22}^p = \frac{E_2^p\,\{(h_c - h)^3 + (-h_c + h + h_p)^3\}}{3(1-\nu_{12}^p \nu_{21}^p)}, \qquad D_{66}^p = \frac{G_{12}^p\,\{(h_c - h)^3 + (-h_c + h + h_p)^3\}}{3},$$

(3.24)

The elements of Eq. (3.20) are

$$A_{11}^{E} = -\frac{E_1^p h_p (d_{31} + \nu_{21}^p d_{32})}{1 - \nu_{12}^p \nu_{21}^p}, \qquad D_{11}^{E} = -\frac{E_1^p h_p (d_{31} + \nu_{21}^p d_{32})(2h + h_p - 2h_c)}{2(1 - \nu_{12}^p \nu_{21}^p)}$$

$$A_{22}^{E} = -\frac{E_2^p h_p (d_{32} + \nu_{12}^p d_{31})}{1 - \nu_{12}^p \nu_{21}^p}, \qquad D_{22}^{E} = -\frac{E_2^p h_p (d_{32} + \nu_{12}^p d_{31})(2h + h_p - 2h_c)}{2(1 - \nu_{12}^p \nu_{21}^p)} \tag{3.25}$$

Note the coupling between the stretching and bending quantities due to nonzero elements B_{ij}^{α} in Eqs. (3.24). In addition, the unimorph actuator produces nonzero in-plane stress resultants as well as nonzero bending moment resultants due to applied voltage.

3.4.4 Bimorph Configuration

In this case, the neutral surface does not shift because the thickness and material properties of the bottom and top piezoelectric layers are taken to be identical. The elements with superscript *t* will be the same as those for the bare shell given in Eq. (3.22). The other elements of Eq. (3.19) are

$$A_{11}^{p} = \frac{2 E_1^p h_p}{1 - \nu_{12}^p \nu_{21}^p}, \qquad A_{12}^{p} = \nu_{21}^p A_{11}^{p}, \qquad A_{22}^{p} = \frac{2 E_2^p h_p}{1 - \nu_{12}^p \nu_{21}^p}, \qquad A_{66}^{t} = 2 G_{12}^p h_p,$$

$$B_{11}^{p} = B_{12}^{p} = B_{22}^{p} = B_{66}^{p} = 0$$

$$D_{11}^{p} = \frac{E_1^p h_p (4 h_p^2 + 6 h_p h + 3h^2)}{6(1 - \nu_{12}^p \nu_{21}^p)}, \qquad D_{12}^{p} = \nu_{21}^p D_{11}^{p},$$

$$D_{22}^{p} = \frac{E_2^p h_p (4h_p^2 + 6h_p h + 3h^2)}{6(1-\nu_{12}^p \nu_{21}^p)}, \qquad D_{66}^{p} = \frac{G_{12}^p h_p (4h_p^2 + 6h_p h + 3h^2)}{6},$$

(3.26)

Due to the two layers of actuators in a bimorph configuration, the elements of Eqs. (3.20) will have to be written separately for the lower and the upper layers. Terms due to the lower layer are

$$A_{11L}^{E} = -\frac{E_1^p h_p (d_{31} + \nu_{21}^p d_{32})}{1-\nu_{12}^p \nu_{21}^p}, \qquad D_{11L}^{E} = \frac{E_1^p h_p (d_{31} + \nu_{21}^p d_{32})(h+h_p)}{2(1-\nu_{12}^p \nu_{21}^p)},$$

$$A_{22L}^{E} = -\frac{E_2^p h_p (d_{32} + \nu_{12}^p d_{31})}{1-\nu_{12}^p \nu_{21}^p}, \qquad D_{22L}^{E} = \frac{E_2^p h_p (d_{32} + \nu_{12}^p d_{31})(h+h_p)}{2(1-\nu_{12}^p \nu_{21}^p)},$$

(3.27)

and the terms due to the upper layer are

$$A_{11U}^{E} = A_{11L}^{E}, \qquad A_{22U}^{E} = A_{22L}^{E}, \qquad D_{11U}^{E} = -D_{11L}^{E}, \qquad D_{22U}^{E} = -D_{22L}^{E}, \qquad (3.28)$$

In the bimorph configuration, the elements B_{ij}^{α} of the coupling matrix are zero because of the symmetric laminate structure. Note from Eqs. (3.27) and (3.28) that if the upper and lower layer actuators are driven by the same voltages (in-phase actuation), the total bending moment resultants due to the two actuators become zero. Similarly, if both the actuators are driven by voltages of the same magnitude but opposite signs (out-of-phase actuation), the in-plane stress resultants of the combination become zero. These characteristics make a bimorph actuator different from a unimorph one and can be advantageous depending upon the application. For example, in-phase driven actuators are shown to couple better into the lower order modes of a circular cylinder (Lester and Lefebvre, 1993).

3.5 Equations of Motion and Actuator Forces

In order to obtain the equivalent distributed actuator forces, we first incorporate the changes in the stresses, Eqs. (3.18), and inertia terms, Eq. (3.16), in the equations of motion presented in the previous chapter, and then separate the terms containing voltages. This yields

$$\frac{1}{A_1A_2}\left[\frac{\partial\{(N_{11}^t+N_{11}^p)A_2}{\partial\alpha_1}+\frac{\partial\{(\tilde{N}_{12}^t+\tilde{N}_{12}^p)A_1}{\partial\alpha_2}+(\tilde{N}_{12}^t+\tilde{N}_{12}^p)\frac{\partial A_1}{\partial\alpha_2}-(N_{22}^t+N_{22}^p)\frac{\partial A_2}{\partial\alpha_1}\right]+\frac{1}{A_1A_2R_1}$$
$$\left[\frac{\partial\{(M_{11}^t+M_{11}^p)A_2\}}{\partial\alpha_1}+\frac{\partial\{(\tilde{M}_{12}^t+\tilde{M}_{12}^p)A_1\}}{\partial\alpha_2}+(\tilde{M}_{12}^t+\tilde{M}_{12}^p)\frac{\partial A_1}{\partial\alpha_2}-(M_{22}^t+M_{22}^p)\frac{\partial A_2}{\partial\alpha_1}\right]+\frac{1}{2A_2}$$
$$\frac{\partial}{\partial\alpha_2}\left[(\tilde{M}_{12}^t+\tilde{M}_{12}^p)\left(\frac{1}{R_1}-\frac{1}{R_2}\right)\right]+N_{11}^r\left(\frac{1}{A_1}\frac{\partial\varepsilon_{11}}{\partial\alpha_1}+\frac{\gamma_{12}}{A_1A_2}\frac{\partial A_1}{\partial\alpha_2}-\frac{\beta_1}{R_1}\right)+2N_{12}^r\left(\frac{1}{A_2}\frac{\partial\varepsilon_{11}}{\partial\alpha_2}-\frac{\gamma_{12}}{A_1A_2}\right.$$
$$\left.\frac{\partial A_2}{\partial\alpha_1}\right)+N_{22}^r\left(\frac{1}{2A_2}\frac{\partial\gamma_{12}}{\partial\alpha_2}+\frac{(\varepsilon_{11}-\varepsilon_{22})}{A_1A_2}\frac{\partial A_2}{\partial\alpha_1}-\frac{1}{A_2}\frac{\partial\beta_n}{\partial\alpha_2}\right)+p\beta_1+q_1+F_1=(\rho h+\Delta_p\rho_p h_p)\ddot{u}_1,$$

$$\frac{1}{A_1A_2}\left[\frac{\partial\{(N_{22}^t+N_{22}^p)A_1\}}{\partial\alpha_2}+\frac{\partial\{(\tilde{N}_{12}^t+\tilde{N}_{12}^p)A_2\}}{\partial\alpha_1}+(\tilde{N}_{12}^t+\tilde{N}_{12}^p)\frac{\partial A_2}{\partial\alpha_1}-(N_{11}^t+N_{11}^p)\frac{\partial A_1}{\partial\alpha_2}\right]+\frac{1}{A_1A_2R_2}$$
$$\left[\frac{\partial\{(M_{22}^t+M_{22}^p)A_1\}}{\partial\alpha_2}+\frac{\partial\{(\tilde{M}_{12}^t+\tilde{M}_{12}^p)A_2\}}{\partial\alpha_1}+(\tilde{M}_{12}^t+\tilde{M}_{12}^p)\frac{\partial A_2}{\partial\alpha_1}-(M_{22}^t+M_{22}^p)\frac{\partial A_1}{\partial\alpha_2}\right]+\frac{1}{2A_1}$$
$$\frac{\partial}{\partial\alpha_1}\left[(\tilde{M}_{12}^t+\tilde{M}_{12}^p)\left(\frac{1}{R_2}-\frac{1}{R_1}\right)\right]+N_{22}^r\left(\frac{1}{A_2}\frac{\partial\varepsilon_{22}}{\partial\alpha_2}+\frac{\gamma_{12}}{A_1A_2}\frac{\partial A_2}{\partial\alpha_1}-\frac{\beta_2}{R_2}\right)+2N_{12}^r\left(\frac{1}{A_1}\frac{\partial\varepsilon_{22}}{\partial\alpha_1}-\frac{\gamma_{12}}{A_1A_2}\right.$$
$$\left.\frac{\partial A_1}{\partial\alpha_2}\right)+N_{11}^r\left(\frac{1}{2A_1}\frac{\partial\gamma_{12}}{\partial\alpha_1}+\frac{(\varepsilon_{22}-\varepsilon_{11})}{A_1A_2}\frac{\partial A_1}{\partial\alpha_2}+\frac{1}{A_1}\frac{\partial\beta_n}{\partial\alpha_1}\right)+p\beta_2+q_2+F_2=(\rho h+\Delta_p\rho_p h_p)\ddot{u}_2,$$

$$\frac{1}{A_1A_2}\frac{\partial}{\partial\alpha_1}\left[\frac{1}{A_1}\left(\frac{\partial\{(M_{11}^t+M_{11}^p)A_2\}}{\partial\alpha_1}+\frac{\partial\{(\widetilde{M}_{12}^t+\widetilde{M}_{12}^p)A_1\}}{\partial\alpha_2}+(\widetilde{M}_{12}^t+\widetilde{M}_{12}^p)\frac{\partial A_1}{\partial\alpha_2}-(M_{22}^t+M_{22}^p)\frac{\partial A_2}{\partial\alpha_1}\right)\right]+\frac{1}{A_1A_2}\frac{\partial}{\partial\alpha_2}\left[\frac{1}{A_2}\left(\frac{\partial\{(M_{22}^t+M_{22}^p)A_1\}}{\partial\alpha_2}+\frac{\partial\{(\widetilde{M}_{12}^t+\widetilde{M}_{12}^p)A_2\}}{\partial\alpha_1}+(\widetilde{M}_{12}^t+\widetilde{M}_{12}^p)\frac{\partial A_2}{\partial\alpha_1}-(M_{11}^t+M_{11}^p)\frac{\partial A_1}{\partial\alpha_2}\right)\right]-\left[\frac{(N_{11}^t+N_{11}^p)}{R_1}+\frac{(N_{22}^t+N_{22}^p)}{R_2}\right]-N_{11}^r\left(\frac{\varepsilon_{11}}{R_1}+\frac{1}{A_1}\frac{\partial\beta_1}{\partial\alpha_1}+\frac{\beta_2}{A_1A_2}\frac{\partial A_1}{\partial\alpha_2}\right)$$
$$-N_{12}^r\left[\frac{1}{A_2}\frac{\partial\beta_1}{\partial\alpha_2}+\frac{1}{A_1}\frac{\partial\beta_2}{\partial\alpha_1}-\frac{\beta_1}{A_1A_2}\frac{\partial A_1}{\partial\alpha_2}-\frac{\beta_2}{A_1A_2}\frac{\partial A_2}{\partial\alpha_1}-\left(\frac{1}{R_1}-\frac{1}{R_2}\right)\beta_n+\left(\frac{1}{R_1}+\frac{1}{R_2}\right)\frac{\gamma_{12}}{2}\right]$$
$$-N_{22}^r\left(\frac{\varepsilon_{22}}{R_2}+\frac{1}{A_2}\frac{\partial\beta_2}{\partial\alpha_2}+\frac{\beta_1}{A_1A_2}\frac{\partial A_2}{\partial\alpha_1}\right)+p(\varepsilon_1+\varepsilon_2)+q_3+F_3=(\rho h+\Delta_p\rho_p h_p)\ddot{w},$$

(3.29)

where the equivalent actuator forces (F_1, F_2, and F_3) due to the applied voltages are given by

$$F_1=\frac{1}{A_1A_2}\left[\frac{\partial(N_{11}^EA_2)}{\partial\alpha_1}-N_{22}^E\frac{\partial A_2}{\partial\alpha_1}+\frac{1}{R_1}\frac{\partial(M_{11}^EA_2)}{\partial\alpha_1}-\frac{M_{22}^E}{R_1}\frac{\partial A_2}{\partial\alpha_1}\right],$$

$$F_2=\frac{1}{A_1A_2}\left[\frac{\partial(N_{22}^EA_1)}{\partial\alpha_2}-N_{11}^E\frac{\partial A_1}{\partial\alpha_2}+\frac{1}{R_2}\frac{\partial(M_{22}^EA_1)}{\partial\alpha_2}-\frac{M_{11}^E}{R_2}\frac{\partial A_1}{\partial\alpha_2}\right],$$

$$F_3=\frac{1}{A_1A_2}\left[\frac{\partial}{\partial\alpha_1}\left\{\frac{1}{A_1}\left(\frac{\partial(M_{11}^EA_2)}{\partial\alpha_1}-M_{22}^E\frac{\partial A_2}{\partial\alpha_1}\right)\right\}+\frac{\partial}{\partial\alpha_2}\left\{\frac{1}{A_2}\left(\frac{\partial(M_{22}^EA_1)}{\partial\alpha_2}-M_{11}^E\frac{\partial A_1}{\partial\alpha_2}\right)\right\}\right]-\left(\frac{N_{11}^E}{R_1}+\frac{N_{22}^E}{R_2}\right)$$

(3.30)

Equations (3.29) describe the equations of motion of a shell under pressure in the presence of piezoelectric patches. These equations take into account the mass and stiffness of the actuators. Equivalent forces, given by Eqs. (3.30), depend upon the applied voltages to the actuators and can be used in controlling the static deflection and vibration of a shell under pressure.

3.6 Distributed Sensing

There exist two basic approaches for calculating the sensor voltage. One approach is to consider an open-circuit configuration in which the total surface charge is assumed to be zero and the sensor voltage is obtained by integrating the electric field over the thickness of the sensor (Tzou, 1993). Another approach is to consider a closed-circuit configuration in which the electric field becomes zero and the total charge on the sensor is obtained by integrating the electric displacement over the sensor area (Lee, 1990; Callahan and Baruh, 1999). The total charge can be divided by the sensor capacitance to get the sensor voltage. Here, we follow the former approach. For a thin piezoelectric patch and considering only the electric field in the transverse direction and open-circuit configuration, one can write the sensor equation as (Tzou, 1993)

$$V_s^m = \frac{1}{Q_s^m} \int_{\alpha_{11}^m}^{\alpha_{12}^m} \int_{\alpha_{21}^m}^{\alpha_{22}^m} \int_{h_{k-1}^m}^{h_k^m} (h_{31}\,\varepsilon_{11}^m + h_{32}\,\varepsilon_{22}^m) A_1 A_2 dz\, d\alpha_1\, d\alpha_2\,, \tag{3.31}$$

where h_{31}, h_{32} are the piezoelectric constants relating the open-circuit voltage to the in-plane normal strains $\varepsilon_{11}^m, \varepsilon_{22}^m$. The symbols Q_s^m and V_s^m stand for the area and output voltage of the m^{th} sensor, respectively. The distances of the lower and the upper surface of the sensor from the reference surface are denoted by h_{k-1}^m and h_k^m, respectively. Similar to the case of an actuator, the coordinates of the m^{th} sensor can be given by the combinations of α_{11}^m, α_{12}^m, α_{21}^m, α_{22}^m. In general, h_{31} will be different from h_{32}. However, due to the

symmetry in the in-plane direction, one can set $h_{31}=h_{32}$ for monolithic sensors. For simplicity, we do not consider geometric nonlinearity in the sensor equation. The sensor equation in terms of displacements can be written as

$$V_s^m = \frac{1}{Q_s^m}\int_{\alpha_{11}^m}^{\alpha_{12}^m}\int_{\alpha_{21}^m}^{\alpha_{22}^m}(h_k^m - h_{k-1}^m)\left[\left\{h_{31}\left(\frac{1}{A_1}\frac{\partial u_1}{\partial \alpha_1}+\frac{u_2}{A_1A_2}\frac{\partial A_1}{\partial \alpha_2}+\frac{w}{R_1}\right)+h_{32}\left(\frac{1}{A_2}\frac{\partial u_2}{\partial \alpha_2}+\frac{u_1}{A_1A_2}\frac{\partial A_2}{\partial \alpha_1}+\right.\right.\right.$$
$$\left.\left.\left.\frac{w}{R_2}\right)\right\}_m+\frac{h_k^m+h_{k-1}^m}{2}\left\{h_{31}\left(\frac{1}{A_1}\frac{\partial \beta_1}{\partial \alpha_1}+\frac{\beta_2}{A_1A_2}\frac{\partial A_1}{\partial \alpha_2}\right)+h_{32}\left(\frac{1}{A_2}\frac{\partial \beta_2}{\partial \alpha_2}+\frac{\beta_1}{A_1A_2}\frac{\partial A_2}{\partial \alpha_1}\right)\right\}_m\right]A_1A_2\,d\alpha_1\,d\alpha_2, \tag{3.32}$$

where the subscript m on the braces denotes the quantity corresponding to the m^{th} sensor. It can be seen from Eq. (3.32) that if we add the sensor voltages obtained from the top and bottom piezoelectric layers of a bimorph, the second term (corresponding to $(h_k^m + h_{k-1}^m)/2$) will vanish. This means that a bimorph sensor cannot sense bending strains. If the unimorph configuration is considered, all terms in Eq. (3.32) will be nonzero in general. Also, as the thickness of the shell and the thickness of the patch decrease, the second term becomes small compared to the first. In other words, the effect of bending strains on the sensor voltage will become smaller in this case. Following the procedure developed for the actuator, one can also take into account the mass and stiffness effects of the sensor.

3.7 State-Space Model

For the convenience of writing, the three equations of motion (Eq. 3.29) can be written in short forms as

$$L_1(u_1,u_2,w) - A_1A_2(\rho h)_{eq}\ddot{u}_1 = F_1,$$
$$L_2(u_1,u_2,w) - A_1A_2(\rho h)_{eq}\ddot{u}_2 = F_2,$$

$$L_3(u_1,u_2,w) - A_1A_2(\rho h)_{eq}\ddot{w} = F_3,$$

(3.33)

where $(\rho h)_{eq}$ is the inertia term of the shell including the piezoelectric patches, F_1, F_2, and F_3 are the generalized forces produced by the actuators, and L_1, L_2, and L_3 are the differential operators describing the equations of motion of the shell in the presence of the patches. Using the modal expansion method, the displacement functions can be written as

$$\{u_1(\alpha_1,\alpha_2,t),u_2(\alpha_1,\alpha_2,t),w(\alpha_1,\alpha_2,t)\} = \sum_{k=1}^{\infty}\eta_k(t)\{U^k(\alpha_1,\alpha_2),V^k(\alpha_1,\alpha_2),W^k(\alpha_1,\alpha_2)\},$$

(3.34)

where $\eta_k(t)$ is the modal participation factor, and $\{U^k(\alpha_1,\alpha_2),V^k(\alpha_1,\alpha_2),W^k(\alpha_1,\alpha_2)\}$ represents the k^{th} mode shape. We substitute the above modal expansion into Eqs. (3.33) and multiply the first, second, and third equations of Eq. (3.33) by $U^p(\alpha_1,\alpha_2)$, $V^p(\alpha_1,\alpha_2)$, and $W^p(\alpha_1,\alpha_2)$, respectively. The superscript p denotes the displacements corresponding to the p^{th} mode shape. Adding the resulting equations and integrating over the whole domain, Ω, we get

$$\begin{aligned}
&\int_{\Omega}\sum_{k=1}^{\infty}[L_1(U^k,V^k,W^k)\eta_k(t)U^p - A_1A_2(\rho h)_{eq}U^k\ddot{\eta}_k(t)U^p + L_2(U^k,V^k,W^k)\eta_k(t)V^p \\
&- A_1A_2(\rho h)_{eq}V^k\ddot{\eta}_k(t)V^p + L_3(U^k,V^k,W^k)\eta_k(t)W^p - A_1A_2(\rho h)_{eq}W^k\ddot{\eta}_k(t)W^p]d\Omega \\
&= \int_{\Omega}[F_1U^p + F_2V^p + F_3W^p]d\Omega.
\end{aligned}$$

(3.35)

Using the properties of mode shapes, we write

$$-\int_{\Omega}[\{\omega_k^2\,\eta_k(t)+\ddot{\eta}_k(t)\}\{(U^k)^2+(V^k)^2+(W^k)^2\}\,A_1A_2(\rho\,h)_{eq}]d\Omega=\int_{\Omega}[F_1U^k+F_2V^k+F_3W^k]d\Omega,$$

(3.36)

where ω_k is the natural frequency of the k^{th} mode. Assuming a modal damping ratio, ζ_k, Eq. (3.36) can be written as

$$\ddot{\eta}_k(t)+2\,\zeta_k\,\omega_k\dot{\eta}_k(t)+\omega_k^2\,\eta_k(t)=f_k, \tag{3.37}$$

where

$$f_k=-\int_{\Omega}[F_1U^k+F_2V^k+F_3W^k]d\Omega\Big/\int_{\Omega}[\{(U^k)^2+(V^k)^2+(W^k)^2\}\,A_1A_2(\rho\,h)_{eq}]d\Omega\,.$$

(3.38)

Equation (3.38) provides the expression for modal force, f_k, that determines how the piezoelectric actuators affect the dynamics in the k^{th} mode. Now we derive an equation to determine how well a particular mode can be sensed using the piezoelectric sensor.

Denoting the term inside the integral sign of Eq. (3.32) by $G_m(u_1,u_2,w)$, and substituting Eq. (3.34), we get the expression for the sensor voltage as

$$V_s^m(t)=\sum_{k=1}^{\infty}\eta_k(t)c_k^m\,, \tag{3.39}$$

where

$$c_k^m=\frac{1}{Q_s^m}\int_{\alpha_{11}^m}^{\alpha_{12}^m}\int_{\alpha_{11}^m}^{\alpha_{12}^m}G_m[U^k(\alpha_1,\alpha_2),V^k(\alpha_1,\alpha_2),W^k(\alpha_1,\alpha_2)]\,A_1A_2d\alpha_1d\alpha_2\,. \tag{3.40}$$

The term c_k^m in Eq. (3.40) is called the modal sensing constant. It determines the contribution of the k^{th} mode shape to the sensor voltage. If, for a particular mode, c_k is zero, the piezoelectric sensor will give no information about the vibration in that particular mode.

From the point of view of vibration control formulation, state-space representation of Eqs. (3.37) and (3.39) is desirable. To this end, we consider *N* modes of vibration and choose the states as $\boldsymbol{x} = \{\dot{\eta}_1, \omega_1 \eta_1, \dot{\eta}_2, \omega_2 \eta_2, \ \ldots \ , \dot{\eta}_N, \omega_N \eta_N\}^T$. Then the state-space model of the vibrating system, Eqs. (3.37) and (3.39), can be written as

$$\dot{\boldsymbol{x}} = \boldsymbol{A}\,\boldsymbol{x} + \boldsymbol{B}\,\boldsymbol{u}, \qquad \boldsymbol{y} = \boldsymbol{C}\,\boldsymbol{x}, \tag{3.41}$$

where $\boldsymbol{u}$ is the actuator voltage, and $\boldsymbol{y}$ is the sensor voltage. The matrices $\boldsymbol{A}$, $\boldsymbol{B}$, and $\boldsymbol{C}$ can be derived appropriately from Eqs. (3.37) and (3.39).

3.8 Conclusions

Actuator and sensor models of piezoelectric patches, attached to a shell vibrating under a constant pressure, were presented. The equations of motions derived for the combination of shell and patch were based upon Sanders' shell theory. The equations took into account stiffness and mass of the patches. The derivations were presented for a non-isotropic active composite material and for both unimorph and bimorph configurations. The resulting equivalent actuator forces generated by piezoelectric patches were given. In addition, a sensor equation was presented based upon an open-circuit configuration. Thereafter, we derived expressions for the effects of actuators and sensors on different modes and presented a state-space model of the system in the modal domain. The equations derived in this chapter will be used in Chapter 5, where we find optimal actuators and sensors, and in Chapter 6, which deals with the vibration control problem.